A study on the adsorption of chromium (VI) from aqueous solutions on the alginate-montmorillonite/polyaniline nanocomposite

Ali Olad*, Fahimeh Farshi Azhar

Polymer Composite Research Laboratory, Faculty of Chemistry, Department of Applied Chemistry, University of Tabriz, P. O. Box: 51665-343, Tabriz, Iran
Tel. +98 411 3393164; Fax: +98 411 3340191; email: a.olad@yahoo.com

ABSTRACT

In this study, batch adsorption system using a novel organic/inorganic hybrid of biopolymer, nanoclay and conducting polymer viz. alginate–montmorillonite/polyaniline (Alg–MMT/PANI) nanocomposite was investigated to describe the adsorption of hexavalent chromium (Cr(VI)) from aqueous solutions. The Alg–MMT/PANI nanocomposite was synthesized by chemical oxidative polymerization of aniline in the presence of alginate-montmorillonite nanocomposite dispersion. The structure and morphology of the prepared nanocomposite was characterized utilizing Fourier transform infrared spectroscopy, X-ray diffraction, and scanning electron microscopy. In the adsorption studies, the effects of initial concentration of Cr(VI), pH, adsorbent dose, and contact time were investigated. Furthermore, the adsorption kinetics studies showed that the adsorption process followed pseudo-second-order model. Also, the investigation of adsorption isotherms revealed that the equilibrium adsorption data were well described by the Freundlich isotherm model. Based on this model, the adsorption capacity, K_f, was calculated to be $29.89\,\mathrm{mg\,g^{-1}}$. Thermodynamic parameters indicated that the adsorption of Cr(VI) by Alg–MMT/PANI nanocomposite is an endothermic process.

Keywords: Alginate; Montmorillonite; Polyaniline; Chromium; Adsorption

1. Introduction

Many heavy metals that are highly toxic for animals and human beings are discharged into the environment as industrial wastes, causing serious soil and water pollution [1]. One of the most important and widely used heavy metals, chromium, is considered as a toxic and carcinogenic environmental pollutant. Chromium exists in the environment as trivalent [Cr(III)] and hexavalent [Cr(VI)] forms. Cr(III) naturally occurs in the environment and is an essential micronutrient for human beings. Conversely, Cr(VI) is about 500 times more hazardous than trivalent one, being carcinogenic and mutagenic to living organisms [2,3]. Due to the environmental concern, the allowed discharge limit of Cr(VI) into inland surface water is $0.1\,\mathrm{mg\,l^{-1}}$ and into the drinking water prescribed by the World Health Organization is $0.05\,\mathrm{mg\,l^{-1}}$. Therefore, Cr(VI) must be substantially removed from

*Corresponding author.

the environment, in order to prevent the harmful effect of Cr(VI) on ecosystems and public health [4]. Main sources of chromium entrance to environment are industrial processes such as electroplating, leather tanning, metal finishing, textile industries, manufacturing of dye, paint and paper [5].

There are various methods to remove Cr(VI) from the solution, such as chemical precipitation [2], chemical reduction [6], electrocoagulation [7], electrochemical reduction [8], supported liquid membrane technique [9], ion exchange [10], Donnan dialysis [11], photocatalytic reduction [12], reverse osmosis [13], and adsorption [14,15]. The chemical precipitation and reduction processes need additional separation techniques for the disposal of high quantities of waste metal residual sludge produced. The major problems of membrane systems for wastewater treatment are membrane scaling, fouling, and blocking. The drawback of the ion-exchange process is the high cost of the resin, while the electrodeposition method is more energy intensive than other methods [2].

Among these methods, adsorption is one of the most economically favorable and technically feasible method to remove Cr(VI) from the solution, and for many years, the effectiveness of various adsorbents has been demonstrated [16–20]. To minimize processing costs, several recent investigations have focused on the use of low-cost and naturally occurring adsorbents for the removal of heavy metals, such as activated carbon [21], coal [22], biopolymers like alginate [23] and chitosan [24], waste materials [25], natural clay minerals such as montmorillonite [26], zeolite [27], and recently, their hybrids with conducting polymers [28–30].

Polyaniline is one of the most important and widely used conducting polymers, which has shown excellent environmental stability and is synthesized at low cost. It is used in many industrial applications, including rechargeable batteries, sensors, magnetic shielding, catalysts, optical applications, and recently in wastewater treatment. Polyaniline can exist in various forms, but its general molecular structure possesses a large amount of amine and imine functional groups, which can interact with some metal ions due to the strong affinity of nitrogen. Based on this characteristic, some researchers have focused toward the application of PANI in heavy metal ions removal from aqueous solutions [31]. For example, reduction of toxic hexavalent chromium in water was successfully carried out by polyaniline powder [30]. In another study, short-chain polyaniline coated on jute fiber is capable of removal and recovery of chromium, as well as reduction of hexavalent to trivalent form in solution [32]. Also PANI and its composites have been explored for the removal of Hg(II) [33] and arsenate [34].

Due to the increasing consciousness of cost-effectiveness and public environmental protection, new composite adsorbents containing PANI and natural resources have attracted much attention. The combination of natural resources and synthetic polymers usefully takes the advantages of the biocompatibility and environmental friendliness of the renewable materials and the physical and mechanical properties of the synthetic components. For instance, Kumar and Chakraborty developed a polyaniline/jute fiber composite adsorbent for Cr(VI) removal [35].

Alginate is a linear polysaccharide biopolymer composed of (1→4)-linked residues of γ-l-guluronic acid (G) and ß-d-mannuronic acid (M). It is used in a wide application area, such as thickener in many food products, pharmaceutical formulations, and textile printing agents. Also alginate has shown a high affinity for metal ions [31], but due to its tendency to swell in water and mechanical weakness, its application in wastewater treatment is limited. To overcome the drawbacks and further increase its adsorptive capacity and mechanical properties, some researchers have interested in the study of alginate composite in recent years. Polymer/clay composite materials have been introduced as new class of polymer composites with special advanced properties. Intercalation of polymer chains into the clay galleries brings improved characteristics to these hybrid materials. In contrast to the high number of studies on polymer/clay composites, the number of studies on biopolymer/clay composite is relatively low. There are few reports on the preparation and properties of alginate-clay composite materials [36,37]. Sodium alginate–montmorillonite composite membranes have been reported for pervaporation dehydration of isopropanol, 1,4-dioxane and tetrahydrofuran [38]. Sodium alginate–magnesium aluminum silicate microcomposite films were prepared for modified-release tablets [39]. However, there is no report on the preparation of hybrid nanocomposite of alginate-clay/polyaniline and its using for the adsorption of heavy metals.

The purpose of this study is to explore a novel adsorbent that have high affinity for Cr(VI) ions. For this, alginate-montmorillonite nanocomposite was prepared, and aniline was polymerized in the media of alginate-montmorillonite through *in situ* polymerization method. The removal of Cr(VI) ions from aqueous solution using the prepared adsorbent in a batch adsorption process was investigated. The behavior of adsorption was examined on effects of the initial Cr(VI) concentration, pH, adsorbent dose, and contact time. Finally, isothermal behavior, kinetic and thermodynamic studies on the adsorption of Cr(VI) were investigated.

2. Experimental procedure

2.1. Materials

Sodium alginate (Alg) used in this study was a laboratory-grade chemicals (Titran, Iran). Sodium montmorillonite KSF (specific surface area = 20–40 m^2/g, cation-exchange capacity = 30 meq/100 g) was obtained from Sigma-Aldrich (USA). Aniline was purchased from Merck and distilled under reduced pressure prior to use. Ammonium peroxydisulfate, hydrochloric acid, sodium hydroxide, and potassium chromate were all obtained from Merck and were used as received without any further purification. Distilled water was used throughout the experiments.

2.2. Instruments

A laboratory pH meter (Inolab pH730, WTW) was used to adjust the pH of the Cr(VI) solution. An ultrasonic probe (Bandelin D-12207, Germany) was used in nanocomposite preparation. Hexavalent chromium concentration was measured by Shimadzu UV-1700 Pharma Spectrophotometer at $\lambda_{max} = 375$ nm wavelength. Fourier transform infrared (FT-IR) spectra were recorded between 400 and 4,000 cm^{-1} using KBr pellets by Bruker, Tensor 27 spectrophotometer. X-ray diffraction patterns (XRD) were collected using a Siemens D500 diffractometer with Cu kα radiation ($\lambda = 1.5418$ Å) at room temperature, operating at a voltage of 35 kV. The XRD patterns were recorded at the scan rate of 1 min^{-1} for a scan range of $2\theta = 2$–70˚. The morphology of the samples was studied using scanning electron microscope (SEM) (LEO 1430 VP, Germany). Each sample was coated with a thin layer of Au-Pd using a sputter coater (Polaron SC7620). Samples were analyzed at 15 kV.

2.3. Preparation of alginate–montmorillonite nanocomposite

An exact amount of alginate (Alg) was dissolved in distilled water to prepare a 2% (w/v) solution. The required amount of Na-MMT (2%, w/v) was dispersed in distilled water for 24 h, and this dispersion was further treated by ultrasonic for 2 min at 30w. Equal volumes of alginate solution and clay dispersion were mixed at 40℃ under agitation. After 8 h of mixing, this solution was poured into polystyrene Petri dishes and was allowed to dry at ambient conditions.

2.4. Synthesis of alginate-montmorillonite/polyaniline nanocomposite

In a typical experiment, to Alg–MMT nanocomposite suspension prepared in Section 2.3, 0.06 mol of aniline dissolved in 75 ml hydrochloric acid (1 M) was added. This mixture was stirred for 15 min using a magnetic stirrer. To this mixture under stirring, ammonium peroxydisulfate (13.68 g) dissolved in 75 ml hydrochloric acid (1 M) was added dropwise at 0–5℃. After completion of the addition, stirring is continued for 6 h. The greenish black powder obtained was washed with distilled water until the filtrate become colorless. Then, the powder was dried in an oven at 60–80℃ for 24 h and used as the adsorbent.

2.5. Batch Cr(VI) adsorption experiments

The Cr(VI) solutions were prepared in different concentrations (30–200 mg l^{-1}) by diluting the stock solution of K$_2$CrO$_4$ (1,000 mg l^{-1}) appropriately as necessary. To determine the conditions that achieve the maximum amount of metal ion removal, batch adsorption experiments were carried out.

Adsorption experiments were carried out using the alginate–montmorillonite/polyaniline (Alg–MMT/PANI) nanocomposite as adsorbent. A known amount of adsorbent was thoroughly mixed at 120 rpm with 25 ml of respective Cr(VI) solutions, with known concentrations and pH values. The pH of the reaction mixture was initially adjusted using either hydrochloric acid (0.1 M) or sodium hydroxide (0.1 M). At the end of desired exposure time, the suspensions were filtered using Whatman filter paper (0.45 mm), and the filtrates were analyzed after complexation with sodium borate for Cr(VI) concentration using UV–Visible spectrophotometer at 375 nm wavelength.

Experimental variables considered were initial concentration of Cr(VI) (30–200 mg l^{-1}), pH (2–9), dosage of nanocomposite (0.01–0.1 mg/25 ml), and contact time between nanocomposite and Cr(VI) (5–3,600 s). For optimizing the adsorption, one parameter was varied at a time keeping the others fixed. Adsorption isotherm studies were carried out with six different initial concentrations (30–200 mg l^{-1}) of Cr(VI). Langmuir and Freundlich models were applied to the adsorption isotherm, and different constants were generated. Kinetic and thermodynamic studies were also conducted in this study.

If q is the amount of metal adsorbed per specific amount of adsorbent (mg g^{-1}), the adsorption capacity at the time t, q_t (mg g^{-1}) is obtained using the Eq. (1):

$$q_t = \frac{(C_i - C_t)\,V}{W} \tag{1}$$

where C_i and C_t (mg l^{-1}) are the concentration of Cr(VI) in solutions at initial and given time t, respectively. V is the solution volume (l) and W is the mass of adsorbent (g).

3. Results and discussion

3.1. Characterization of Alg–MMT and Alg–MMT/PANI nanocomposites

FT-IR provides specific information about chemical bonding and molecular structures. In this study, FT-IR analysis was applied to examine the possible interactions between the components of the nanocomposite. The FT-IR spectra of Alg, MMT, PANI, Alg–MMT, and Alg–MMT/PANI nanocomposites are shown in Fig. 1. FT-IR spectrum of Alg exhibited absorption bands at $3,415\,cm^{-1}$ (OH stretching), $2,931\,cm^{-1}$ (CH_2 stretching), $1,618\,cm^{-1}$ (COO^- asymmetric stretching), and $1,412\,cm^{-1}$ (COO^- symmetric stretching). The bands at $900–1,200\,cm^{-1}$ are due to the O–C–O stretching of ether groups and the –C–O stretching of alcoholic groups [40]. FT-IR spectrum of Na–MMT showed the band at $460\,cm^{-1}$ due to Si-O-Si deformation, the band at $524\,cm^{-1}$ due to Si–O–Al deforma-tion, the band at $1,031\,cm^{-1}$ due to Si–O stretching, the band at $1,633\,cm^{-1}$ due to OH deformation of H_2O, the band at $3,433\,cm^{-1}$ due to O–H stretching of H_2O, and the band at $3,624\,cm^{-1}$ due to the stretching mode of OH band in the inner surfaces of Na–MMT [41]. The main characteristic absorption bands of pure PANI were observed at $3,414\,cm^{-1}$ (N–H stretching vibration), $1,550\,cm^{-1}$ (C=C stretching of the quinoid ring), $1,460\,cm^{-1}$ (C=C stretching of the benzenoid ring), $1,230$ and $1,286\,cm^{-1}$ (C–N stretching), and $790\,cm^{-1}$ (C–H stretching) [27]. In the FT-IR spectrum of Alg–MMT, incorporation of clay in Alg matrix decreased the intensity of CH_2 stretching peaks. While the absorption wavelength of the COO peaks does not change with the loading of MMT clay to alginate. Moreover, in the spectrum of Alg–MMT/PANI, the presence of absorption bands of three components with a little shift confirmed the preparation of hybrid nanocomposite.
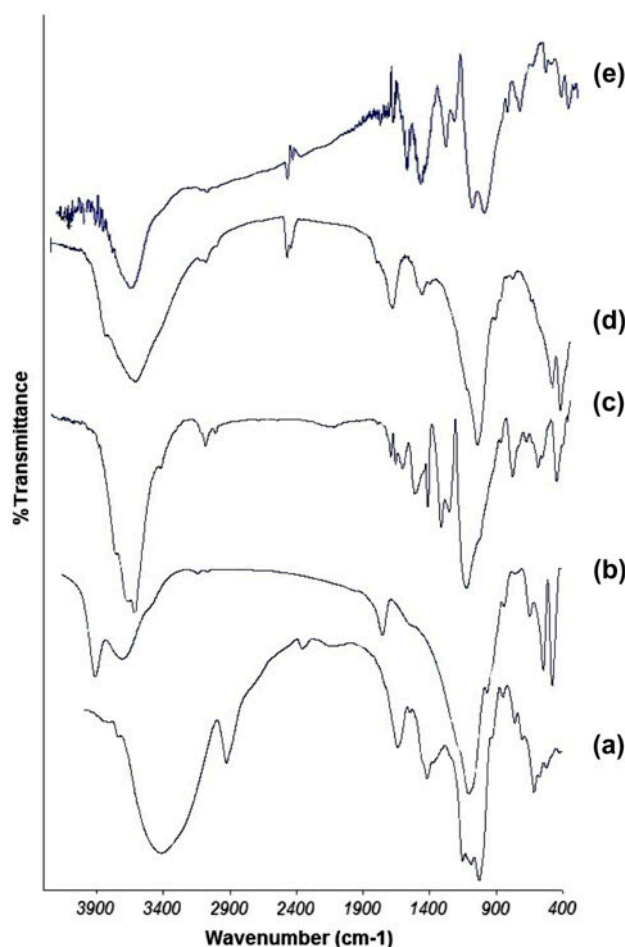
XRD is a versatile and nondestructive technique that is used for identification of the crystalline phases present in solid materials and analyzing the structural properties. Fig. 2 shows the XRD of Alg, MMT, PANI, Alg–MMT, and Alg–MMT/PANI nanocomposites. The diffraction peaks of the Alg are at $2\theta = 19.01°$, $31.72°$, $33.89°$, and $45.44°$. Pure MMT revealed its characteristic peak at $2\theta = 7.03°$, which is corresponding to a d-spacing of $12.55\,\text{Å}$ (From the diffraction peak, d-spacing can be determined using Bragg's equation; $n\lambda = 2d \sin \theta$). The XRD pattern of PANI indicates its less crystalline structure. The diffraction peaks at $2\theta = 20.64°$, $25.52°$, and $26.18°$ were assigned to the emeraldine polyaniline. The peak at $2\theta = 25.52°$ is corresponding to the periodicity parallel and perpendicular to polyaniline chains [42]. In the case of Alg–MMT, the characteristic peak related to clay ($2\theta = 7.03°$) was shifted to lower degree ($2\theta = 5.31°$), indicating the intercalation of alginate into the silicate galleries and confirmation of intercalated Alg–MMT nanocomposite. The XRD pattern of Alg–MMT/PANI showed characteristic peak of Alg–MMT nanocomposite but with less intensity and less sharpness because of introducing amorphous PANI, which confirms the formation of Alg–MMT/PANI nanocomposite.

The morphologies of pristine alginate, montmorillonite, polyaniline, Alg–MMT and Alg–MMT/PANI nanocomposites were investigated by scanning electron microscopy. The SEM images of the samples are shown in Fig. 3(a)–(e). The SEM micrograph for alginate (Fig. 3(a)) revealed irregular spherical granules in the size range of $5–45\,\mu m$, and the surface was quite smooth. From the SEM image of the original montmorillonite (Fig. 3(b)), we can see that the MMT layers are overlapped together. SEM image of polyaniline

Fig. 1. FT-IR spectra of (a) alginate, (b) montmorillonite, (c) polyaniline, (d) Alg–MMT nanocomposite, and (e) Alg–MMT/PANI nanocomposite.
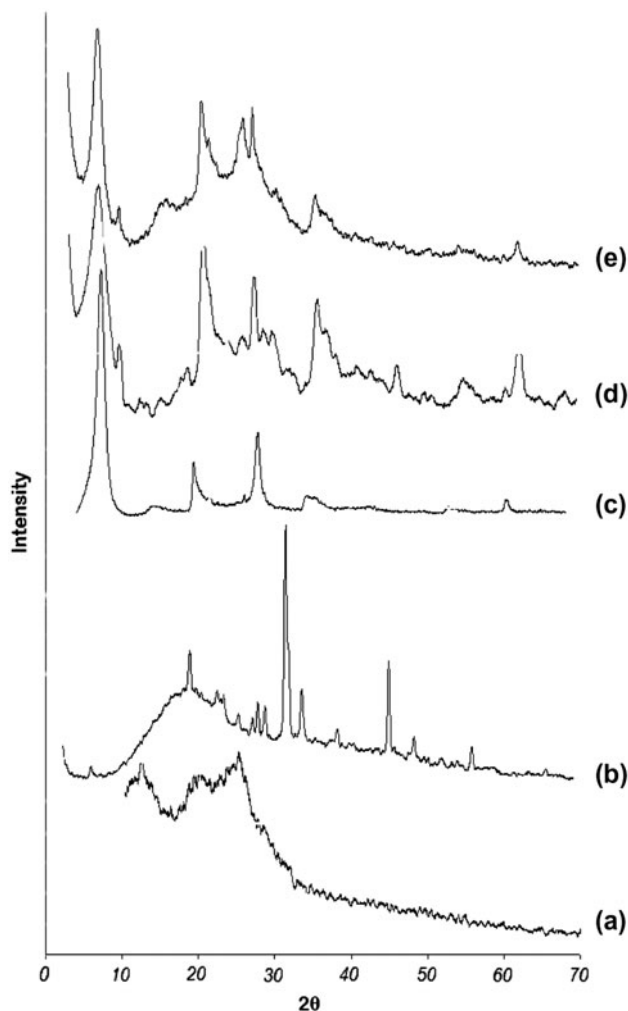
Fig. 2. XRD of (a) polyaniline, (b) alginate, (c) montmorillonite, (d) Alg–MMT nanocomposite, and (e) Alg–MMT/PANI nanocomposite.

showed a globular morphology with a particle diameter less than 100 nm (Fig. 3(c)). After intercalation of alginate into the montmorillonite layers, the granular structure of alginate had changed to a fracture surface and the Alg–MMT nanocomposites displayed an oriented fracture probably due to the orientation of the crystal clay layered into the alginate matrix (Fig. 3(d)). Fig. 3(e) shows the SEM image of Alg–MMT/PANI nanocomposite. It is evident that the surface of the Alg–MMT/PANI nanocomposite is rough than that observed in case of Alg–MMT nanocomposite. This is indicative of the fact that polymerization of aniline is taking place over the surface of the Alg–MMT nanocomposite causing to the formation of a layer on the surface of Alg–MMT nanocomposite. This roughness provides a good possibility for Cr(VI) to be adsorbed. The size of the particles was varied from 80 to 110 nm.

3.2. Effect of adsorbent

The adsorption of Cr(VI) from aqueous solutions by various adsorbents (Alg–MMT, Alg/PANI and Alg–MMT/PANI) was evaluated. 0.05 g of adsorbents was exposed to the 25 ml of Cr(VI) solution with the initial concentration of 50 mg l^{-1}. After 800 s exposure time, the adsorption capacities of Cr(VI) by mentioned adsorbents were compared (Fig. 4). Minimum adsorption capacity is obtained by using Alg–MMT nanocomposite. This is due to the intercalation of alginate in the silicate layers of montmorillonite which prevents chromium penetrating into MMT layers. In the case of Alg/PANI composite, polymerization of aniline on the surface of the alginate creates a porous surface which leads to a better adsorption capacity for Cr(VI) removal. Maximum adsorption capacity is achieved by using Alg–MMT/PANI nanocomposite. It was found that MMT/PANI has the synergetic effect in the adsorption and removal of Cr(VI). From SEM results, it is indicative that the intercalation of alginate in the silicate layers of MMT and polymerization of aniline over the surface of the Alg–MMT nanocomposite causes to the formation of a large rough surface area. This roughness provides a good possibility for Cr(VI) to be adsorbed.

3.3. Effect of initial Cr(VI) concentration

The effect of initial concentration of Cr(VI) solution on the adsorption of Cr(VI) by Alg–MMT/PANI nanocomposite was investigated. For this, 0.05 g of nanocomposite was exposed to the 25 ml of Cr(VI) solutions with various initial concentrations of 30–200 mg l^{-1} at pH = 9 and 25°C temperature. Fig. 5 shows the adsorption capacity of Cr(VI) on Alg–MMT/PANI nanocomposite after 200 s of exposure. The results revealed that the amount of Cr(VI) adsorbed per unit mass of the adsorbent is increased with an increase in initial Cr(VI) concentration. This may be due to the high driving force for mass at a high initial Cr(VI) concentration. In other words, the residual concentration of Cr(VI) will be higher for higher initial Cr(VI) concentrations. In the case of lower concentrations, the ratio of initial number of Cr(VI) ions to the available adsorption sites is low, and subsequently, the fractional adsorption becomes independent of initial concentration [43].

3.4. Effect of pH

The pH of the aqueous solution is an important parameter in the adsorption process and affects on the interaction between the adsorbent and adsorbate.
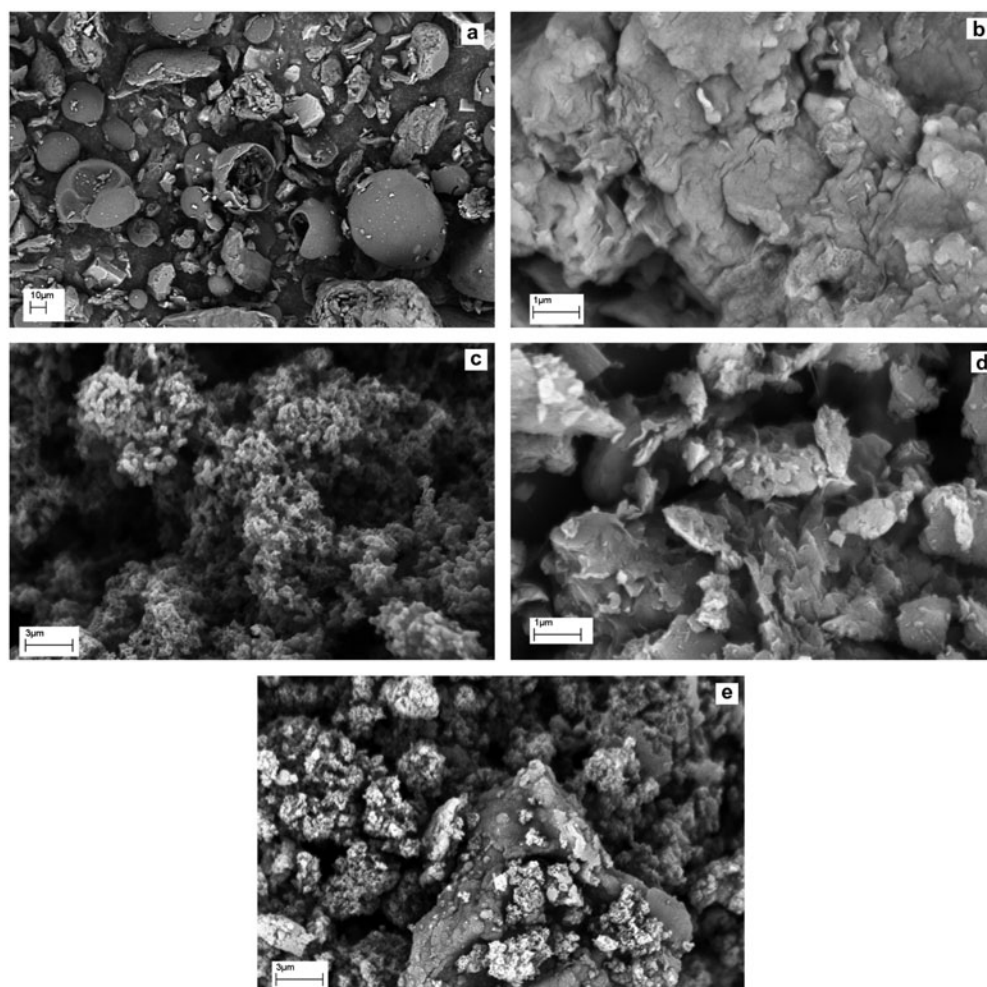
Fig. 3. SEM images of (a) alginate, (b) montmorillonite, (c) polyaniline, (d) Alg–MMT nanocomposite, and (e) Alg–MMT/PANI nanocomposite.
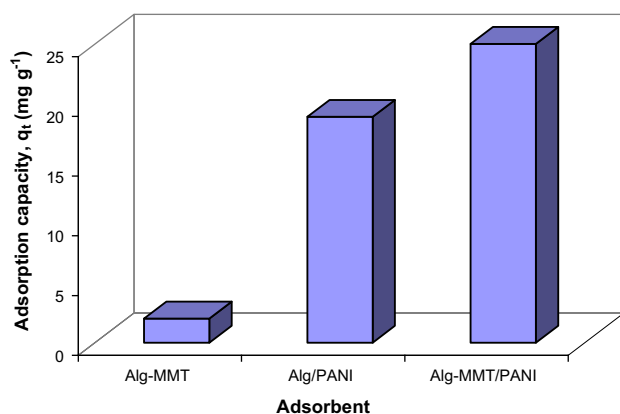
Fig. 4. Effect of adsorbent on the adsorption capacity of Cr(VI) by Alg–MMT/PANI nanocomposite at concentration of Cr(VI) $(50 \, mg \, l^{-1})$, pH = 9, adsorbent dose (0.05 g), batch volume (25 ml), temperature (25℃), 120 rpm.
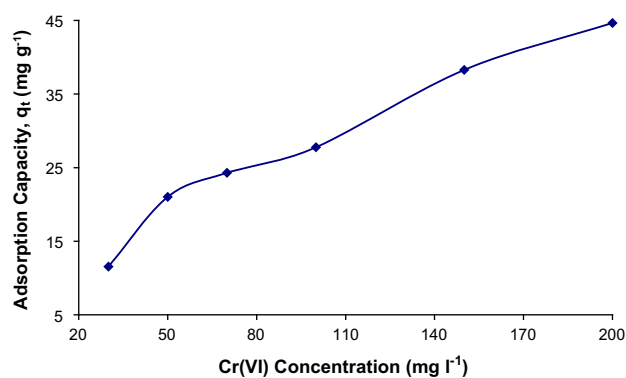
Fig. 5. Effect of initial concentration of Cr(VI) on the adsorption capacity of Cr(VI) by Alg–MMT/PANI nanocomposite, pH = 9, adsorbent dose (0.05 g), batch volume (25 ml), temperature (25℃), contact time (5 min), 120 rpm.

The effect of the initial solution pH on the Cr(VI) adsorption was studied at 25℃; 0.05 g of Alg–MMT/PANI nanocomposite was contacted to the 25 ml of Cr(VI) solution with the initial concentration of 50 mg l^{-1} with different pH in the rang 2–9. After 10 s of exposure, the adsorption capacity was determined (Fig. 6). It was found that the maximum adsorption capacity onto nanocomposite is occurred at the pH rang of 2–4 and the adsorption decreased by the increasing of pH from 4 to 7. Very low adsorption capacities were observed at pH values higher than 7. The effect of pH on the Cr(VI) adsorption is related to the surface charge of the adsorbent and different complexes that Cr(VI) can form in aqueous solutions with different pH values [2,31].

In acidic media (pH < 4), protonation of the nanocomposite nitrogen atoms is occurred. Also, the predominant form of Cr(VI) at acidic pH values is oxyanion forms such as CrO_4^{2-} and $Cr_2O_7^{2-}$. So a strong attraction is made between the oxyanions of Cr(VI) and the positively charged surface of the adsorbent. As a result, the adsorption occurs through the electrostatic interaction between the two counterions. However, as the pH increases (4–9) deprotonation of nitrogen atoms of the nanocomposite was occurred, leading to the depletion of active sites in the adsorbent. Therefore, the interaction of nanocomposite with the Cr(VI) is hindered and consequently results in the lower uptake.

3.5. Effect of adsorbent dosage

The effect of Alg–MMT/PANI nanocomposite amount on the Cr(VI) adsorption capacity was studied

at 25℃. Various amounts of nanocomposite were contacted to the 25 ml of Cr(VI) solutions with the initial concentration of 50 mg l^{-1} and after 60 s the adsorption capacities were calculated. From Fig. 7, it can be seen that the adsorption capacity decreased with increasing the amount of nanocomposite. The primary reason is that adsorption sites remain unsaturated during the adsorption process, whereas the number of sites available for adsorption increases by increasing the adsorbent amount [44]. Thus, future experiments were carried out using 0.01 g of adsorbent per 25 ml of Cr(VI) solution.

3.6. Adsorption isotherm

Adsorption isotherms are important for the description of how adsorbate interacts with adsorbent surface. In the present study, two well-known isotherm equations viz. Langmuir [45] and Freundlich [46] isotherms have been applied for explanation of the adsorption data. The Langmuir isotherm is valid for monolayer sorption due to a surface of a finite number of identical sites and assumes that uptake of metal ions occurs on a homogenous surface without any interaction between adsorbed ions. This isotherm expressed in the linear form as Eq. (2):

$$\frac{C_e}{q_e} = \frac{1}{bQ_0} + \frac{C_e}{Q_0} \tag{2}$$

where C_e is the equilibrium concentration (mg l^{-1}) and q_e the amount adsorbed at equilibrium (mg g^{-1}). The Langmuir constants Q_0 (mg g^{-1}) represent the monolayer adsorption capacity and b (l mg^{-1}) relates the heat of adsorption.

Fig. 6. Effect of pH on the adsorption capacity of Cr(VI) by Alg–MMT/PANI nanocomposite at concentration of Cr(VI) (50 mg l^{-1}), adsorbent dose (0.05 g), batch volume (25 ml), temperature (25℃), contact time (10 s), 120 rpm.
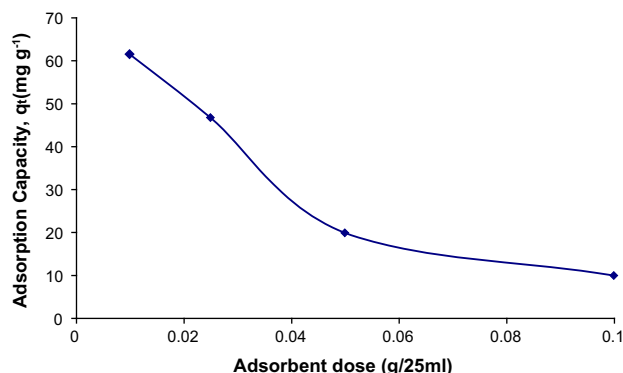
Fig. 7. Effect of adsorbent dose on the adsorption capacity of Cr(VI) by Alg–MMT/PANI nanocomposite at concentration of Cr(VI) (50 mg l^{-1}), pH = 2, batch volume (25 ml), temperature (25℃), contact time (1 min), 120 rpm.

The essential feature of the Langmuir adsorption can be expressed by means of R_L, a dimensionless constant referred to as separation factor for predicting whether an adsorption system is favorable or unfavorable. R_L is calculated using Eq. (3):

$$R_L = \frac{1}{1 + bC_0} \tag{3}$$

where C_0 is the initial concentration (mg l^{-1}). The parameter R_L indicates the favorability of the adsorption as below:

(1) $R_L > 1$, unfavorable adsorption.
(2) $0 < R_L < 1$, favorable adsorption.
(3) $R_L = 0$, irreversible adsorption.
(4) $R_L = 1$, linear adsorption.

The Freundlich isotherm describes the heterogeneous surface energies by multilayer adsorption and is expressed in linear form as Eq. (4):

$$\ln q_e = \ln K_f + \left(\frac{1}{n}\right) \ln C_e \tag{4}$$

where K_f (mg g^{-1}) is approximately an indicator of the adsorption capacity, and $1/n$ is the adsorption intensity and an indicator for the favorability of adsorption. As the values of $n > 1$ represents favorable adsorption condition [47].

In this study, the Langmuir and Freundlich isotherms for the adsorption of Cr(VI) onto Alg–MMT/PANI nanocomposite were studied at two different temperatures, 25 and 55℃; 0.01 g of nanocomposite was exposed to the 25 ml of Cr(VI) solutions with various initial concentrations of 30–200 mg l^{-1} at pH = 2. After 600 s, the isotherm parameters were calculated using Eqs. (2) and (4), and the detailed parameters of

adsorption isotherms are listed in Table 1. The results showed that both the isotherms fit almost well with the experimental values suggesting a physio-chemical interaction of chromium ions with the adsorbents. But the equilibrium data fitted to Freundlich model better than Langmuir model indicating multilayer adsorption. Based on Freundlich model, the adsorption capacity, K_f, was calculated to be 29.89 mg g^{-1}.

The Langmuir constant Q_0 and Freundlich constant K_f values increased with increasing temperature implying that the adsorption process was endothermic in nature. The value of Langmuir constant b and Freundlich constant n also increased with temperature suggesting that the Cr(VI) exhibited higher affinity for the nanocomposite at higher temperature. The value of R_L in Langmuir model has been found to be 0.44 and 0.39 at 25℃ and 55℃, respectively, showing that the adsorption of Cr(VI) on adsorbent is favorable. In Freundlich model, n values are 1.69 and 1.74 at 25℃ and 55℃, respectively, both greater than unity indicated that the adsorption of Cr(VI) onto the nanocomposite was favorable.

3.7. Effect of contact time

The effect of contact time between the Alg–MMT/PANI nanocomposites and Cr(VI) solution was studied at 25℃. 0.01 g of adsorbent was contacted to the 25 ml of Cr(VI) solution with the initial concentration of 50 mg l^{-1} at pH = 2 and 25℃ temperature. The adsorption capacities determined at different contact time intervals (Fig. 8). Results indicated that the adsorption capacity was increased within 900 s and remains almost constant even up to an hour. This may be due to the fact that once certain amount of Cr(VI) adsorbed onto nanocomposite within a given

Table 1
Langmuir and Freundlich isotherm constants for the adsorption of Cr(VI) on Alg–MMT/PANI nanocomposite

Isotherm	Constants	Alg–MMT/PANI Temperature	
		25℃	55℃
Langmuir	R^2	0.9022	0.9724
	Q_0	370.37	476.19
	b	0.0251	0.0307
	R_L	0.44	0.39
Freundlich	R^2	0.9016	0.9960
	n	1.6934	1.7406
	K_f	19.7365	29.8893
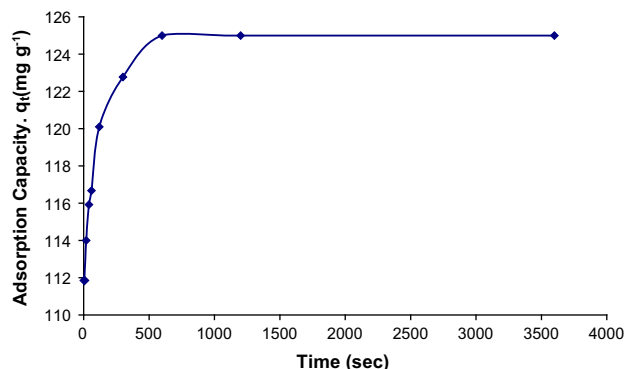
Fig. 8. Effect of contact time on the adsorption capacity of Cr(VI) by Alg–MMT/PANI nanocomposite at concentration of Cr(VI) (50 mg l^{-1}), pH = 2, adsorbent dose (0.01 g), batch volume (25 ml), temperature (25℃), 120 rpm.

Table 2
Values of the parameters of kinetic models for the adsorption of Cr(VI) on Alg–MMT/PANI nanocomposite

Cr(VI) (mg l^{-1})	Lagergren		Pseudo second order		Second order	
	R^2	K_L (min^{-1})	R^2	K' (g mg^{-1} min^{-1})	R^2	K_2 (g mg^{-1} min^{-1})
50	0.9608	2.76×10^{-3}	0.9954	3.32×10^{-4}	0.9885	1.00×10^{-3}

Table 3
Thermodynamic parameters for the adsorption of Cr(VI) on Alg–MMT/PANI nanocomposite

Temperature (K)	ΔG (kJ mol^{-1})	ΔH (kJ mol^{-1})	ΔS (J mol^{-1})
298.15	−3.25	25.49	96.39
328.15	−4.46		91.27

time, no more adsorption occurs afterwards. Further, the achievement of maximum adsorption level within 15 min suggests that a very minimum contact time is sufficient enough for the removal of Cr(VI) from solution by this nanocomposite.

3.8. Adsorption kinetics

The kinetic parameters are helpful for the prediction of adsorption rate, which gives important information for the efficiency of adsorption [47]. For kinetics studies of Cr(VI) adsorption, 0.01 g of the Alg–MMT/PANI nanocomposite was exposed to the 25 ml of Cr(VI) solution with initial concentration of 50 mg l^{-1} at pH = 2 and 25°C temperature. According to the Figure 8, adsorption of Cr(VI) attained a maximum after 900 s and thereafter was almost constant up to the studied time of 3,600 s. Therefore, it can be concluded that the rate of Cr(VI) binding with adsorbent was greater in the initial stages, then gradually decreased and remained almost constant. The first rapid increase in binding capacity is due to the presence of vacant site available at the initial time. Generally, when adsorption involves a surface reaction process, the initial adsorption is rapid. Then, a slower adsorption would follow as the available adsorption site gradually decreases.

In this study, in order to determine the best kinetic model which fits the adsorption experimental data, the Lagergren-first-order, the pseudo-second-order, and the second-order models according to Eqs. (5–7), were examined.

$$\log \frac{(q_e - q_t)}{q_e} = \log q_e - \frac{K_L}{2.303} t \tag{5}$$

$$\frac{t}{q_t} = \frac{1}{K' q_e^2} + \frac{t}{q_e} \tag{6}$$

$$\frac{1}{q_e - q_t} = \frac{1}{q_e} + K_2 t \tag{7}$$

where K_L is the Lagergren-first-order rate constant (min^{-1}); K' the pseudo-second-order rate constant (g mg^{-1} min^{-1}) and K_2 the second-order rate constant (g mg^{-1} min^{-1}); q_e and q_t are the amounts of metal adsorbed (mg g^{-1}) at equilibrium and at time t, respectively. The kinetic parameters of Cr(VI) adsorption onto Alg–MMT/PANI nanocomposite are reported in Table 2. Results showed that the kinetic data fitted best into pseudo-second-order model as reported for other biopolymeric material [48]. The correlation coefficient (R^2) and rate constant obtained from the pseudo-second-order model were 0.9954 and 3.32×10^{-4}, respectively.

3.9. Adsorption thermodynamics

The values of thermodynamic parameters are relevant for the practical application of adsorption process. Isotherm data related to the adsorption of Cr(VI) onto the Alg–MMT/PANI nanocomposite at 25°C and 55°C were analyzed to obtain the values of thermodynamic parameters. Change in free energy (ΔG), enthalpy (ΔH), and entropy (ΔS) for the adsorption process were determined using Eqs. (8–11) [48,49] and calculated values are listed in Table 3.

$$K_c = \frac{C_{Ac}}{C_e} \tag{8}$$

$$\Delta G = -2.303 \, RT \log K_c \tag{9}$$

Table 4
Comparison of adsorption capacity of Cr(VI) on Alg–MMT/PANI nanocomposite with different adsorption systems

Adsorbents	Model	Adsorption capacity (mg g^{-1})	References
PANI-PEG composite	Freundlich	0.68	[16]
Activated alumina	Freundlich	0.956	[18]
Timber industry waste	Freundlich	1.84	[25]
Wheat shell	Freundlich	1.9288	[17]
Carboxy methyl cellulose	Langmuir	5.1	[50]
PANI/zeolite nanocomposite	Freundlich	5.97	[1]
Chitosan cross-linked with epichlorohydrin	Langmuir	11.3	[51]
HPAM-chitosan gel beads	Langmuir	13.34	[19]
Olive stones	Freundlich	18.10	[52]
Poly(o-toluidine)/pumice	Langmuir	19.4	[53]
Modified chitosan bentonite	Langmuir	22.17	[20]
Wood apple shell	Langmuir	28.81	[54]
Alg–MMT/PANI nanocomposite	Freundlich	29.89	This study
Kapok fiber-oriented-PANI nanofibers	Freundlich	33.25	[4]

$$\frac{\ln b_2}{\ln b_1} = \frac{-\Delta H}{R}\left(\frac{1}{T_2} - \frac{1}{T_1}\right)$$ (10)

$$\Delta G = \Delta H - T\Delta S$$ (11)

where K_c is the equilibrium constant, C_{Ac} and C_e are equilibrium concentrations (mg l^{-1}) of Cr(VI) on the Alg–MMT/PANI nanocomposite and in the solution, respectively. ΔG change in Gibbs free energy (J mol^{-1}), R universal gas constant (8.314 J K^{-1} mol^{-1}), T, T_1, and T_2 temperatures (K), ΔH change in enthalpy (J mol^{-1}), b_1 and b_2 are Langmuir constants at temperatures T_1 and T_2, respectively. ΔS Change in entropy (J mol^{-1} K^{-1}).

Negative values of ΔG indicated that the adsorption process was favorable and spontaneous in nature. It may be noted that with the increase in temperature from 25 to 55℃ the value of ΔG decreased from −3.25 to −4.46 kJ mol^{-1}. Thus, adsorption of Cr(VI) onto the nanocomposite was increased at higher temperature. The positive value of enthalpy change (ΔH) confirmed the endothermic nature of the adsorption process. Positive values of ΔS suggested good affinity of the metal ion toward the adsorbent and increased randomness at the solid–solution interface during the fixation of the metal ion on the active site of the adsorbent.

3.10. Comparison of adsorption capacity with other systems

An interesting comparison between the adsorption capacity of the Alg–MMT/PANI nanocomposite on

the basis of Freundlich adsorption capacity (K_f, mg g^{-1}), and other adsorbents are presented in Table 4. In comparing our results with the results reported in the literature, it can be concluded that the Alg–MMT/PANI nanocomposite exhibits higher affinity for Cr(VI) compared with many other adsorbents from earlier reports.

3.11. Desorption studies

To make the adsorbent economically competitive, the prepared nanocomposite should be reused for
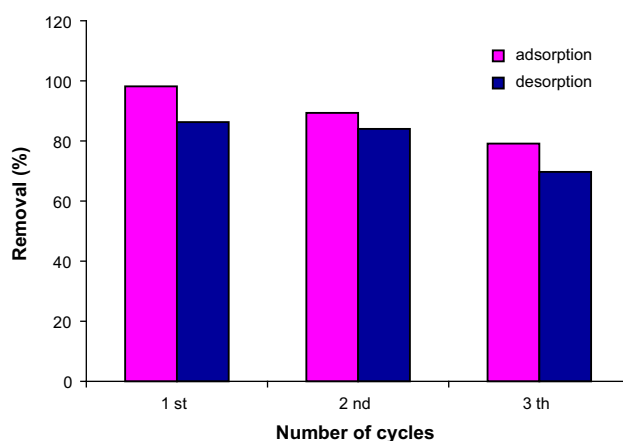
Fig. 9. Adsorption/desorption cycles of the removal of chromium ions by Alg–MMT/PANI nanocomposite at concentration of Cr(VI) (50 mg l^{-1}), pH = 2, adsorbent dose (0.01 g), batch volume (25 ml), temperature (25℃), contact time for adsorption (1 min), contact time for desorption (2 h), 120 rpm.

"*n*" number of cycles. For desorption studies, 0.01 g of the Alg–MMT/PANI nanocomposite was exposed to the 25 ml of Cr(VI) solution with initial concentrations of $50\,mg\,l^{-1}$ at pH = 2 and 25°C temperature. Contact time for adsorption experiments was 60 s, and 98.14% of the Cr(VI) was removed in the 1st cycle of adsorption. Adsorbed Cr(VI) could be stripped by the introduction of protons that competed with metal ions for binding sites. The used nanocomposite was treated with 0.3 M oxalic acid for 7,200 s which resulted into 86.4% stripping of Cr(VI) in the 1st cycle of desorption. The adsorption ability was almost completely resumed after the regeneration of acid-treated sorbent. In the second cycle of adsorption, the adsorbent could remove 89.32% Cr(VI) that could be desorbed up to 84.04%. In the third cycle, 79.14% adsorption and 69.7% desorption were possible (Fig. 9). The removal decreased nominally per cycle up to third cycle suggesting very high efficiency of the adsorbent. In the last cycle, 79.14% adsorption was feasible.

4. Conclusion

The synthesis of Alg–MMT/PANI nanocomposite was performed by chemical oxidative polymerization of aniline in the presence of alginate-montmorillonite nanocomposite dispersion. The application of prepared nanocomposite was investigated as an adsorbent for the removal of Cr(VI) from aqueous solutions. Lower pH and higher temperature values were found as the favorable conditions for maximum Cr(VI) adsorption. The equilibrium data from experiments were analyzed by the Langmuir and Freundlich models that showed better fit with Freundlich model. The adsorption capacity, K_f, from this model was found to be $29.88\,mg\,g^{-1}$. The batch sorption kinetics was tested and the pseudo-second-order kinetic model was able to best describe the adsorption kinetic of the Cr(VI) onto Alg–MMT/PANI nanocomposite. The thermodynamics of the system pointed out that the adsorption process was endothermic. Finally, the novel nanocomposite designed in this study is distinguished by significantly higher adsorption capability, reusability, stability, and versatile applicability making it an industrially viable, economical and successful product to removal of Cr(VI) ions from solutions.

Acknowledgments

References

[1] A.A. Hasan, O.A. Shyaa, A.M. Abbas, Synthesis and characterization of polyaniline/zeolite nanocomposite for the removal of chromium(VI) from aqueous solution, J. Saudi Chem. Soc. (in press). doi:10.1016/j.jscs.2012.01.001

[2] A.G. Yavuz, E. Dincturk-Atalay, A. Uygun, F. Gode, E. Aslan, A comparison study of adsorption of Cr(VI) from aqueous solutions onto alkyl-substituted polyaniline/chitosan composites, Desalination 279 (2011) 325–331.

[3] M. Sankır, S. Bozkır, B. Aran, Preparation and performance analysis of novel nanocomposite copolymer membranes for Cr(VI) removal from aqueous solutions, Desalination 251 (2010) 131–136.

[4] Y. Zheng, W. Wang, D. Huang, A. Wang, Kapok fiber oriented-polyaniline nanofibers for efficient Cr(VI) removal, Chem. Eng. J. 191 (2012) 154–161.

[5] A.K. Meena, K. Kadirvelu, G.K. Mishra, C. Rajagopal, P.N. Nagar, Adsorptive removal of heavy metals from aqueous solution by treated sawdust, J. Hazard. Mater. 150 (2008) 604–611.

[6] L. Alidokht, A.R. Khataee, A. Reyhanitabar, S. Oustan, Reductive removal of Cr(VI) by starch-stabilized Fe⁰ nanoparticles in aqueous solution, Desalination 270 (2011) 105–110.

[7] T. Olmez, The optimization of Cr(VI) reduction and removal by electrocoagulation using response surface methodology, J. Hazard. Mater. 162 (2009) 1371–1378.

[8] P. Lakshmipathiraj, G.B. Raju, M.R. Basariya, S. Parvathy, S. Prabhakar, Removal of Cr(VI) by electrochemical reduction, Sep. Purif. Technol. 60 (2008) 96–102.

[9] R. Guell, E. Antico, V. Salvado, C. Fontàs, Efficient hollow fiber supported liquid membrane system for the removal and pre concentration of Cr(VI) at trace levels, Sep. Purif. Technol. 62 (2008) 389–393.

[10] F. Gode, E. Pehlivan, Removal of Cr(VI) from aqueous solution by two Lewatitanion exchange resins, J. Hazard. Mater. B 119 (2005) 175–182.

[11] T. Sardohan, E. Kir, A. Gulec, Y. Cengeloglu, Removal of Cr (III) and Cr(VI) through the plasma modified and unmodified ion-exchange membranes, Sep. Purif. Technol. 74 (2010) 14–20.

[12] J.K. Yang, S.M. Lee, Removal of Cr(VI) and humic acid by using TiO2 photo-catalysis, Chemosphere 63 (2006) 1677–1684.

[13] C. Das, P. Patel, S. De, S. Das Gupta, Treatment of tanning effluent using nanofiltration followed by reverse osmosis, Sep. Purif. Technol. 50 (2006) 291–299.

[14] E.S. Abdel-Halim, S.S. Al-Deyab, Hydrogel from crosslinked polyacrylamide/guar gum graft copolymer for sorption of hexavalent chromium ion, Carbohydr. Polym. 86 (2011) 1306–1312.

[15] Q. Li, Y. Qian, H. Cui, Q. Zhang, R. Tang, J. Zhai, Preparation of poly(aniline-1,8- diaminonaphthalene) and its application as adsorbent for selective removal of Cr(VI) ions, Chem. Eng. J. 173 (2011) 715–721.

[16] M. Riahi Samani, S.M. Borghei, A. Olad, M.J. Chaichi, Removal of chromium from aqueous solution using polyaniline-poly ethylene glycol composite, J. Hazard. Mater. 184 (2010) 248–254.

[17] P. Das Saha, A. Dey, P. Marik, Batch removal of chromium (VI) from aqueous solutions using wheat shell as adsorbent: Process optimization using response surface methodology, Desalin. Water Treat. 39 (2012) 95–102.

[18] I. Marzouk, C. Hannachi, L. Dammak, B. Hamrouni, Removal of chromium by adsorption on activated alumina, Desalin. Water Treat. 26 (2011) 279–286.

[19] W. Kuang, Y. Tan, L. Fu, Adsorption kinetics and adsorption isotherm studies of chromium from aqueous solutions by HPAM-chitosan gel beads, Desalin. Water Treat. 45 (2012) 222–228.

[20] R. Huang, B. Yang, B. Wang, D. Zheng, Z. Zhang, Removal of chromium (VI) ions from aqueous solutions by N-2-hydroxypropyl trimethyl ammonium chloride chitosan–bentonite, Desalin. Water Treat. 50 (2012) 329–337.

[21] L. Monser, N. Adhoum, Modified activated carbon for the removal of copper, zinc, chromium and cyanide from waste-water, Sep. Purif. Technol. 26 (2002) 137–146.

[22] F. Gode, E. Moral, Column study on the adsorption of Cr(III) and Cr(VI) using Pumice, Yarıkkaya brown coal, Chelex-100 and Lewatit MP 62, Bioresour. Technol. 99 (2008) 1981–1991.

[23] H.A. Shawky, Improvement of water quality using alginate/montmorillonite composite beads, J. Appl. Polym. Sci. 119 (2011) 2371–2378.

[24] K.Z. Elwakeel, Environmental application of chitosan resins for the treatment of water and wastewater: A review, J. Dispersion Sci. Technol. 31 (2010) 273–288.

[25] M. Bansal, D. Singh, V.K. Garg, Chromium (VI) uptake from aqueous solution by adsorption onto timber industry waste, Desalin. Water Treat. 12 (2009) 238–246.

[26] S.S. Gupta, K.G. Bhattacharyya, Interaction of metal ions with clays: I. A case study with Pb(II), Appl. Clay Sci. 30 (2005) 199–208.

[27] A. Olad, M. Khatamian, B. Naseri, Removal of toxic hexavalent chromium by polyaniline modified clinoptilolite nanoparticles, J. Iran. Chem. Soc. 8 (2011) S141–S151.

[28] M. Ghorbani, M. Soleimani Lashkenari, H. Eisazadeh, Application of polyaniline nanocomposite coated on rice husk ash for removal of Hg(II) from aqueous media, Synth. Met. 161 (2011) 1430–1433.

[29] D. Shao, C. Chen, X. Wang, Application of polyaniline and multiwalled carbon nanotube magnetic composites for removal of Pb(II), Chem. Eng. J. 185–186 (2012) 144–150.

[30] A. Olad, R. Nabavi, Application of polyaniline for the reduction of toxic Cr(VI) in water, J. Hazard. Mater. 147 (2007) 845–851.

[31] N. Jiang, Y. Xu, Y. Dai, W. Luo, L. Dai, Polyaniline nanofibers assembled on alginate microsphere for Cu²⁺ and Pb²⁺ uptake, J. Hazard. Mater. 215–216 (2012) 17–24.

[32] P.A. Kumar, S. Chakraborty, M. Ray, Removal and recovery of chromium from wastewater using short chain polyaniline synthesized on jute fiber, Chem. Eng. J. 141 (2008) 130–140.

[33] J. Wang, B. Deng, H. Chen, X. Wang, J. Zheng, Removal of aqueous Hg(II) by polyaniline: Sorption characteristics and mechanisms, Environ. Sci. Technol. 43 (2009) 5223–5228.

[34] L. Yang, S. Wu, J.P. Chen, Modification of activated carbon by polyaniline for enhanced adsorption of aqueous arsenate, Ind. Eng. Chem. Res. 46 (2007) 2133–2140.

[35] P.A. Kumar, S. Chakraborty, Fixed-bed column study for hexavalent chromium removal and recovery by short-chain polyaniline synthesized on jute fiber, J. Hazard. Mater. 162 (2009) 1086–1098.

[36] F. Tezcan, E. Gunister, G. Ozen, F.B. Erim, Biocomposite films based on alginate and organically modified clay, Int. J. Biol. Macromol. 50 (2012) 1165–1168.

[37] J.M. Vale, R.S. Justice, D.W. Schaefer, J.E. Mark, Calcium alginate barrier films modified by montmorillonite clay, J. Macromol. Sci. Phys. 44 (2005) 821–831.

[38] S.D. Bhat, T.M. Aminabhavi, Novel sodium alginate–Na⁺MMT hybrid composite membranes for pervaporation dehydration of isopropanol, 1,4-dioxane and tetrahydrofuran, Sep. Purif. Technol. 51 (2006) 85–94.

[39] T. Pongjanyakul, A. Priprem, S. Puttipipatkhachorn, Investigation of novel alginate–magnesium aluminum silicate microcomposite films for modified-release tablets, J. Control. Release 107 (2005) 343–356.

[40] Y. Vijaya, S.R. Popuri, V.M. Boddu, A. Krishnaiah, Modified chitosan and calcium alginate biopolymer sorbents for removal of nickel (II) through adsorption, Carbohydr. Polym. 72 (2008) 261–271.

[41] G.V. Joshi, B.D. Kevadiya, H.A. Patel, H.C. Bajaj, R.V. Jasra, Montmorillonite as a drug delivery system: Intercalation and in vitro release of timolol maleate, Int. J. Pharm. 374 (2009) 53–57.

[42] V. Janaki, K. Vijayaraghavan, B.T. Oh, K.J. Lee, K. Muthuchelian, A.K. Ramasamy, S. Kamala-Kannan, Starch/polyaniline nanocomposite for enhanced removal of reactive dyes from synthetic effluent, Carbohydr. Polym. 90 (2012) 1437–1444.

[43] A. Rashidzadeh, A. Olad, Novel polyaniline/poly (vinyl alcohol)/clinoptilolite nanocomposite: Dye removal, kinetic, and isotherm studies, Desalin. Water Treat. (in press). doi:10.1080/19443994.2013.766904

[44] F. Ghorbani, H. Younesi, S.M. Ghasempouri, A.A. Zinatizadeh, M. Amini, A. Daneshi, Application of response surface methodology for optimization of cadmium adsorption in an aqueous solution by Saccharomyces cerevisiae, Chem. Eng. J. 145 (2008) 267–275.

[45] I. Langmuir, Adsorption of gaseous on plane surface of glass, mica and platinum, J. Am. Chem. Soc. 40 (1918) 1361–1403.

[46] H.M.F. Freundlich, Over the adsorption in solution, Z. Phys. Chem. 57 (1906) 385–470.

[47] H.-Y. Zhu, Y.-Q. Fu, R. Jiang, J. Yao, L. Xiao, G.-M. Zeng, Novel magnetic chitosan/poly(vinyl alcohol) hydrogel beads: preparation, characterization and application for adsorption of dye from aqueous solution, Bioresour. Technol. 105 (2012) 24–30.

[48] S. Pandey, S.B. Mishra, Organic–inorganic hybrid of chitosan/organoclay bionanocomposites for hexavalent chromium uptake, J. Colloid Interface Sci. 361 (2011) 509–520.

[49] M. Kumar, B.P. Tripathi, V.K. Shahi, Crosslinked chitosan/polyvinyl alcohol blend beads for removal and recovery of Cd(II) from wastewater, J. Hazard. Mater. 172 (2009) 1041–1048.

[50] M.Y. Arıca, G. Bayramoglu, Cr(VI) biosorption from aqueous solutions using free and immobilized biomass of Lentinus sajor-caju: Preparation and kinetic characterization, Colloid Surf. A 253 (2005) 203–211.

[51] S. Qian, G. Huang, J. Jiang, F. He, Y. Wang, Studies of adsorption behavior of crosslinked chitosan for Cr(VI), Se(VI), J. Appl. Polym. Sci. 77 (2000) 3216–3219.

[52] K. Rouibah, A.-H. Meniai, L. Deffous, M. Bencheikh Lehocine, Chromium VI and cadmium II removal from aqueous solutions by olive stones, Desalin. Water Treat. 16 (2010) 393–401.

[53] A.U. Gok, F. Gode, Composites of poly(2-chloroaniline) and poly(o-toluidine) with pumice and their application in the removal of chromium(VI) ions from aqueous solutions, J. Appl. Polym. Sci. 107 (2008) 2295–2303.

[54] K.M. Doke, M. Yusufi, R.D. Joseph, E.M. Khan, Biosorption of hexavalent chromium onto wood apple shell: equilibrium, kinetic and thermodynamic studies, Desalin. Water Treat. 50 (2012) 170–179.